



HAL
open science

Non-local geometric phase in two-photon interferometry

Anthony Martin, Olivier Alibart, Jean-Christoph Flesch, Joseph Samuel,
Supurna Sinha, Sébastien Tanzilli, Anders Kastberg

► To cite this version:

Anthony Martin, Olivier Alibart, Jean-Christoph Flesch, Joseph Samuel, Supurna Sinha, et al.. Non-local geometric phase in two-photon interferometry. EPL - Europhysics Letters, 2012, 97, pp.10003. 10.1209/0295-5075/97/10003 . hal-00614759v1

HAL Id: hal-00614759

<https://hal.science/hal-00614759v1>

Submitted on 3 Oct 2011 (v1), last revised 4 Jan 2012 (v2)

HAL is a multi-disciplinary open access archive for the deposit and dissemination of scientific research documents, whether they are published or not. The documents may come from teaching and research institutions in France or abroad, or from public or private research centers.

L'archive ouverte pluridisciplinaire **HAL**, est destinée au dépôt et à la diffusion de documents scientifiques de niveau recherche, publiés ou non, émanant des établissements d'enseignement et de recherche français ou étrangers, des laboratoires publics ou privés.

Nonlocal Geometric Phase Measurements in Polarized Interferometry with Pairs of single Photons

A. Martin¹, O. Alibert¹, J.-C. Flesch¹, J. Samuel², Supurna Sinha², S. Tanzilli¹, and A. Kastberg^{1,2}

¹Laboratoire de Physique de la Matière Condensée, CNRS UMR 6622, Université de Nice – Sophia Antipolis, Parc Valrose, Nice Cedex 2, France

²Raman Research Institute, Bangalore 560 080, India

We report the experimental observation of the nonlocal geometric phase in Hanbury Brown-Twiss polarized intensity interferometry. The experiment involves two independent, polarized, incoherent sources, illuminating two polarized detectors. Varying the relative polarization angle between the detectors introduces a geometric phase equal to half the solid angle on the Poincaré sphere traced out by a *pair* of single photons. Local measurements at either detector do not reveal the effect of the geometric phase, which appears only in the coincidence counts between the two detectors, showing a genuinely nonlocal effect. We show experimentally that coincidence rates of photon arrival times at separated detectors can be controlled by the two photon geometric phase. This effect can be used for manipulating and controlling photonic entanglement.

PACS numbers: 03.65.Vf, 42.50.-p, 42.50.Ar, 42.25.Ja

Quantum interference is one of the most delicate and intriguing aspects of quantum theory. A subtle interference effect, discovered surprisingly late, is due to the geometric phase [1, 2]. It was soon realized [3] that Berry's discovery had been anticipated by Pancharatnam's work on the interference of polarized light [4]. Pancharatnam's work is now widely recognized as an early precursor and optical analog of the geometric phase [3, 5].

Studies of the geometric phase usually deal with *amplitude* interferometry, which describes the interference of particles from coherent sources. Of particular interest to us here are multiparticle interference effects, discovered by Hanbury Brown and Twiss (HB-T), who performed *intensity* interferometry experiments using incoherent thermal sources [6]. In a previous paper [7], an experiment was proposed to detect a nonlocal Pancharatnam phase in polarized intensity interferometry. The idea of the experiment, *c.f.* Fig. 1, is to have two thermal sources of opposite circular polarizations, P_R and P_L , where R and L describe right and left hand circular polarizations respectively. These illuminate two detectors that are covered by linear polarization analyzers, P_3 and P_4 . A theoretical analysis of the experiment reveals that as the relative angle between the two linear polarizations, φ_{34} , is changed, the rate of coincidence counts between the arrival time of photons at the two detectors varies sinusoidally [7].

Entanglement lies at the very heart of quantum physics. It is now widely recognized as a fundamental resource in the growing field of quantum information, regarding both quantum computation and communication protocols [8, 9]. As with any resource, effective use requires control, and quantum information applications are especially concerned with the degree of entanglement between spatially separated quantum channels or systems.

A multiparticle Aharonov-Bohm effect was discussed theoretically by Büttiker [10] who noted in the context of electronic charge transport that two-particle correla-

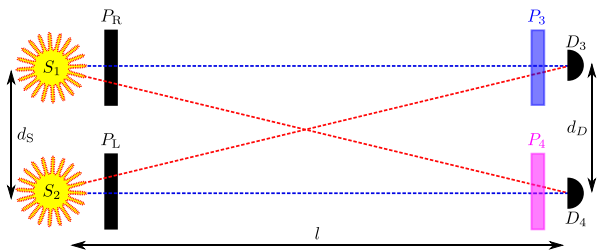


FIG. 1. General scheme for the Pancharatnam phase dependent two-photon intensity interferometry.

tions can be sensitive to a magnetic flux even if the single particle observables are flux insensitive. The effect of the flux is visible only in current cross correlations and is a genuinely nonlocal and multiparticle Aharonov-Bohm effect [11]. This has been experimentally seen in intensity interferometry experiments carried out using edge currents in quantum Hall systems [12], and the theory is further developed in [13, 14]. These authors propose an experiment in which Aharonov-Bohm fluxes may be used to control the orbital entanglement of electronic states. While this proposal is sound in principle, in practice, such experiments may be afflicted by decoherence [8, 9]. In contrast to electronic states, photonic states are easier to generate, manipulate and distribute. Most studies related to quantum communication protocols use photons rather than massive particles. However, photons are neutral and unaffected by the magnetic fields needed in the Aharonov Bohm effect. The idea here is to use the geometric phase as an effective magnetic field to control the degree of photonic entanglement [7].

As a step towards achieving this goal, we report in this letter an experiment based on two independent polarized thermal sources for a demonstration of the nonlocal Pancharatnam phase effect. Such a nonlocal effect can only be observed in the intensity correlations $\mathcal{G}^{(2)}$. A previ-

ously reported experiment involving single photons prepared in mixed polarization states led to lower order correlations $\mathcal{G}^{(1)}$ [15]. Here we take advantage of the setup suggested in [7] and show that the geometric phase effect only appears in the coincidence counts between spatially separated detectors when the relative angle between the polarization analysers is tuned. The two photon Pancharatnam phase is nonlocal in the precise sense that it cannot be observed when local measurements at either detector are performed. The coincidence counts between the two detectors are modulated by a phase which has a geometric component as well as a dynamical (or propagation) phase.

Ideally, the experiment should use *a priori* incoherent thermal sources, as in the HB-T experiment. However, natural thermal light sources would necessitate very short integration times (shorter than the coherence time), which is hard to implement experimentally. Standard laser sources, which are usually used in amplitude interferometry, are unsuitable since they are coherent and do not show the HB-T effect. In this experiment, we use a laser source and introduce incoherence by passing the laser beam through a ground glass plate [16]. This gives us a source of light in which the amplitude and phase are randomly varying, mimicking a thermal light source intensity distribution. Using such a (pseudo-thermal) source, we demonstrate the nonlocal Pancharatnam phase [7].

The central quantity of interest is the polarized intensity-intensity correlation function measured by the coincidence counts for the detectors D_3 and D_4 , given by:

$$\mathcal{C} = \mathcal{G}_{34}^{(2)} = \frac{\langle N_3 N_4 \rangle}{\langle N_3 \rangle \langle N_4 \rangle}, \quad (1)$$

N_3 and N_4 being the photon numbers detected at D_3 and D_4 per time per bandwidth. The detailed theory is outlined in [7]. The theoretical prediction for \mathcal{C} in the limit $l \gg d_S, d_D$ is:

$$\mathcal{C} = \frac{3}{2} + \frac{1}{2} \cos \left[\mathbf{d}_D \cdot (\mathbf{k}_2 - \mathbf{k}_1) + \frac{\Omega}{2} \right], \quad (2)$$

where $\mathbf{k}_i = k \hat{r}_i$ is the wavevector of light seen in the i^{th} detector.

This theoretical calculation can be summarized as follows. There is a process in which a photon from S_1 reaches detector D_3 and a photon from S_2 reaches D_4 (direct process, shown in blue). There is also a corresponding exchange process in which a photon from S_1 reaches D_4 and one from S_2 reaches D_3 (exchange process, shown in red). These two processes are indistinguishable, and in the absence of any ‘welcherweg’ information, we have to combine the amplitudes for these processes with a relative phase ϕ , which depends on the optical path difference between the two processes. The quantum interference between these processes causes the HB-T effect. Only the

interference between direct and exchange processes gives rise to oscillations; the remaining terms providing the background of 1 in $\mathcal{G}^{(2)}$. We expect that the coincidence counts should vary with the propagation phases and thus, the counts should depend on the detector separation d_D and the wavelength λ of the light. The new effect that is present in this polarized version of HB-T is that the coincidence counts also depend on the difference between the linear polarization angles for P_3 and P_4 , φ_{34} , and is modulated by a geometric phase of half the solid angle Ω covered on the Poincaré sphere by the four polarizations involved (see Fig. 2). The closed path on the Poincaré sphere is a property of a *pair* of photons. Each photon by itself does not enclose a solid angle. The effect of the geometric phase on the coincidence rates of photons at the detectors D_3 and D_4 is what we measure in the experiment below.

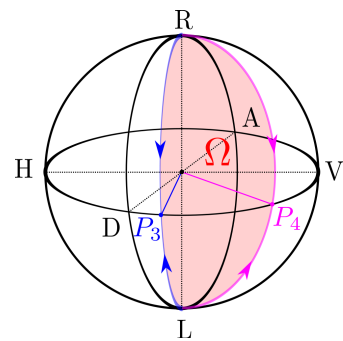


FIG. 2. Path on the Poincaré sphere determining the detected geometric phase. The relative angle φ_{34} between the linear polarizers P_3 and P_4 sets the angular width of the enclosed surface on the sphere. $\Omega = 4\varphi_{34}$ corresponds to the solid angle defined by the geodesic path $R \rightarrow P_3 \rightarrow L \rightarrow P_4 \rightarrow R$.

Our experimental realization of Fig. 1 is schematically shown in Fig. 3. Two independent pseudo-thermal light sources (S_1 and S_2) are spatially filtered using single mode fibers, and their polarizations are adjusted to right-hand and left-hand circular (P_R and P_L for S_1 and S_2 , respectively) using polarizing beamsplitters (PBS) and quarter-wave plates. The output photons from the sources are first directed towards a set of non-polarizing beamsplitters (BS) in order to split each source into two paths. The four resulting paths are led towards the linear polarization analyzers P_3 and P_4 . A second set of BS is then used to recombine, before each analyzer, two paths, with identical probability amplitudes, emanating from S_1 and S_2 . The linear analyzers are each a half-waveplate and a PBS, and the detectors are two independent silicon avalanche photodiodes (APD), featuring 5% detection efficiencies and dark count rates on the order of 100/s.

Our pseudo-thermal sources emit monochromatic, thermal light, with an adjustable coherence time. This is accomplished by focusing a 852 nm external cavity diode laser on a rotating, ground glass disk, producing

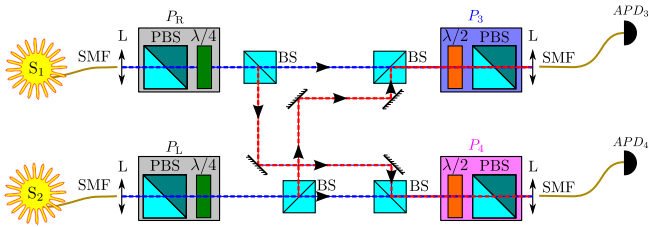


FIG. 3. Experimental setup for demonstrating the Pancharatnam phase at the single photon level. S_1 and S_2 : independent pseudo-thermal light sources; SMF: single-mode optical fibre; L: lens; PBS: polarizing beamsplitter; $\lambda/4$ and $\lambda/2$: quarter- and half-waveplates, respectively; BS: non-polarizing beam-splitter; APD: avalanche photodiode.

time dependent fluctuations in the beam [17, 18]. The scattered light is then collected using two single-mode optical fibers, which provide suitable spatial mode selections. The light arrives at the observation point, P, scattered through different routes. The electric field intensity received can be written as a sum over scatterers $E = \sum_i E_i \exp(i\phi_i)$, where the phase ϕ_i and the amplitude E_i due to the i^{th} scatterer are both random. The statistics of the intensity fluctuations is given by a Rayleigh distribution [16, 19]

$$P(I) = \frac{1}{I_0} \exp\left(-\frac{I}{I_0}\right). \quad (3)$$

The light received at P becomes uncorrelated with itself as the beam traverses the plate. For a Gaussian beam profile incident on the glass plate, we expect the intensity autocorrelation function $\mathcal{G}^{(2)}(\tau) = \langle I(0)I(\tau) \rangle / (\langle I(0) \rangle \langle I(0) \rangle)$ to show a Gaussian decay in time [19]. More precisely, $\mathcal{G}^{(2)}(\tau) = 1 + \exp(-\pi(\tau/\tau_c)^2)$, where the coherence time τ_c is on the order of the time taken by a point on the glass plate to traverse the beam width. Such a Gaussian decay of correlations is indeed observed in our experiment.

The average intensities have been chosen such that both the probability of having more than one photon during the dead-time of the APDs (45 ns), and the probability of having a dark count, are negligible. The effective coherence times of the sources, and the absence of correlations between them, have been tested by measuring their autocorrelations ($\mathcal{G}_{ii}^{(2)}(\tau)$) and the crosscorrelation function ($\mathcal{G}_{ij}^{(2)}(\tau)$). The corresponding experimental results are shown in Fig. 4. As predicted, both sources feature a Gaussian correlation decay as a function of time, associated with coherence times of about 7-800 μs . In addition they exhibit no crosscorrelation, proving they are actually independent. Therefore, we have estimated that sampling frequencies down to 100 kHz will ensure good measurements of $\mathcal{G}^{(2)}(0)$, while 10^5 samples give us a negligible error. These parameters have been chosen in order to minimize the measurement time, and thus

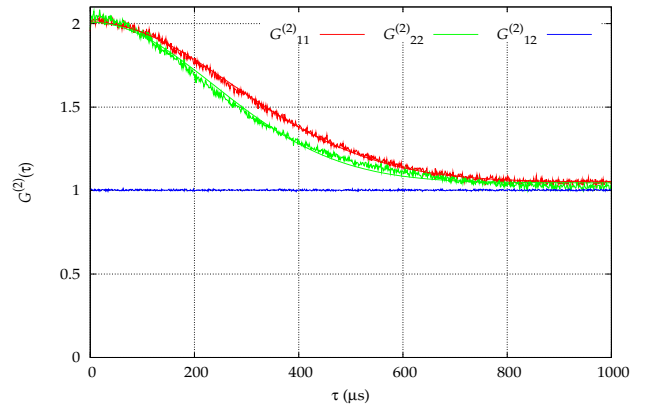


FIG. 4. Autocorrelation functions ($\mathcal{G}_{11}^{(2)}(\tau)$ and $\mathcal{G}_{22}^{(2)}(\tau)$) of the pseudo-thermal light sources S_1 and S_2 (red and green), and their crosscorrelation function ($\mathcal{G}_{12}^{(2)}(\tau)$ – blue), as functions of time using sampling frequency of 1 MHz.

avoiding any unwanted path length fluctuations in the interferometer, as well as frequency drifts of the laser.

To observe the interference pattern in the coincidence counts \mathcal{C} (see Eq. 2), we rotate the P_3 analyzer's half-waveplate by an angle θ from 0 to 2π , thereby continuously scanning the polarization (and thus the angle φ_{34} , from 0 to 4π). The recorded signal is shown in Fig. 5, as well as the expected fringe pattern with an ideal visibility.

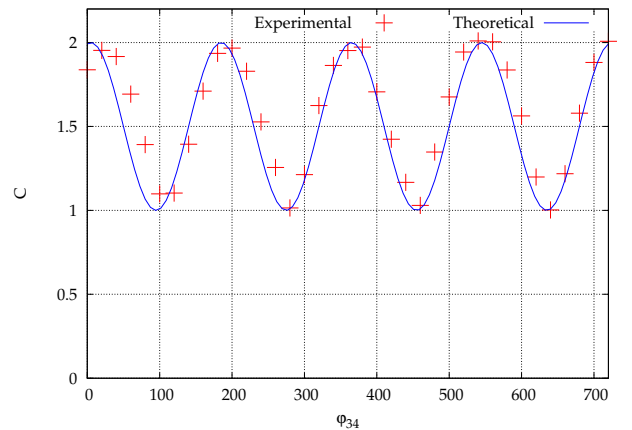


FIG. 5. Crosscorrelation function $\mathcal{C} = \mathcal{G}_{34}^{(2)}(0)$, as function of the angle $\varphi_{34} = 2\theta$ between the polarizations P_3 and P_4 .

Apart from its intrinsic interest as a demonstration of the nonlocal geometric phase in optics, one of our prime motivations is to realize a controllable and reconfigurable circuit enabling the generation and the manipulation of all the four photonic entangled Bell states [9]. This can be done by extending our experiment in the following way. Let us first replace the two thermal sources of Fig. 1 by two simultaneously heralded single photon sources.

We suppose that when two photons are emitted at the same time, *i.e.*, one per source, they have opposite circular polarization. Second, we interface these polarized single photon emitters and the current setup by a time-bin preparation circuit acting on the two photons [8]. This way, using beamsplitters and identical delay lines for the two photons, we can make these photons travel over short, $|s\rangle$, or long, $|l\rangle$, paths, with certain probability amplitudes, and accordingly prepare time-bin input qubits for the geometric phase setup. We prepare incident photons initially with P_R and P_L polarization in the time-bin superpositions $|\varphi\rangle = \alpha|s\rangle + \beta|l\rangle$ and $|\psi\rangle = \alpha'|s\rangle + \beta'|l\rangle$, respectively. Here, α , β , α' , and β' are complex numbers related to the beamsplitting ratios. In this configuration [18], the output state is given by:

$$|\Upsilon\rangle = \frac{1}{\sqrt{2}} (|\varphi_3\rangle|\psi_4\rangle + e^{i\phi}|\psi_3\rangle|\varphi_4\rangle), \quad (4)$$

where ϕ can be tuned using the geometric phase.

On one hand, simply setting the input states to $|\varphi\rangle = |s\rangle$ and $|\psi\rangle = |l\rangle$ permits preparing time-bin entangled states of the form $(|sl\rangle + e^{i\phi}|ls\rangle)/\sqrt{2}$. Such states are otherwise non trivial to produce with usual experimental means based on pulsed parametric down-conversion associated with a preparation interferometer [20]. Here, the geometric phase allows switching between the $|\Psi^+\rangle$ and the $|\Psi^-\rangle$ Bell states.

On the other hand, substituting in Eq. 4 superposition input states of the form $|\varphi\rangle = (|s\rangle + e^{i\phi_1}|l\rangle)/\sqrt{2}$ and $|\psi\rangle = (|s\rangle + e^{i\phi_2}|l\rangle)/\sqrt{2}$, where ϕ_1 and ϕ_2 are the relative phases between short and long time-bin paths for either photon, leads to:

$$|\Upsilon\rangle = \frac{1}{\sqrt{2}} \left[|\Phi(\pi + 2\phi_1)\rangle \cos \frac{\phi}{2} + e^{\frac{i}{2}(\phi + \pi + 2\phi_1)} |\Psi^-\rangle \sin \frac{\phi}{2} \right], \quad (5)$$

in which we have set $\phi_2 = \pi + \phi_1$. By setting $\phi = 0$, and changing the two other phases, we have access to any superposition of $|\Phi^-\rangle$ and $|\Phi^+\rangle$, and to these two basis states as well. This simple scheme therefore leads to the possibility of acting on and/or controlling the degree of entanglement. Regarding experimental realizations, note that the heralded photon sources and the entanglement preparation and control circuits could be realized in the near future using integrated optics, as discussed in [21]. This would make our scheme particularly suitable for practical realizations.

In the example above entanglement is generated by particle exchange effects rather than by interactions. The latter degree of entanglement can be quantified either using Bell's inequality or by the von Neumann entropy of the reduced density matrix, after tracing over one of the subsystems (3 or 4). A straightforward calculation of the von Neumann entropy shows that it does depend on

the geometric phase. Since the geometric phase is achromatic, we can apply the same phase over all the frequencies in the band of interest by tuning φ_{34} and generate entangled photon pairs with the degree of accuracy and the control needed for a source of photonic entanglement.

To conclude, we have experimentally demonstrated a simple generalization of the HB-T effect, making use of the vector nature of light in order to produce a geometric phase. The only conceptual difference between the proposed experiment and the classic HB-T experiment is the presence of polarizers at the sources and detectors. These polarizers cause a geometric phase to appear in the coincidence counts between the two detectors that receive linearly polarized light. Neither the single count rates, nor the self correlations of individual detectors show any geometric phase effects. These appear solely in the *cross* correlation between the count rates of the detectors. This experimental demonstration will open up possibilities for entanglement tuning via the geometric phase.

We acknowledge support from the CNRS, the University of Nice - Sophia Antipolis, the Agence Nationale de la Recherche (ANR) for the 'e-QUANET' project (grant agreement ANR-09-BLAN-0333-01), the European ICT-2009.8.0 FET Open program for the 'QUANTIP' project (grant agreement 244026), and the Conseil Regional PACA, for financial support.

-
- [1] M. V. Berry, Proc. Roy. Soc. Lond. **392**, 45 (1984).
 - [2] A. Shapere and F. Wilczek, *Geometric Phases in Physics* (World Scientific, Singapore, 1989).
 - [3] S. Ramaseshan and R. Nityananda, Curr. Sci. **55**, 1225 (1986).
 - [4] S. Pancharatnam, Proc. Indian Acad. Sci. **44**, 247 (1956).
 - [5] J. Samuel and R. Bhandari, Phys. Rev. Lett. **60**, 2339 (1988).
 - [6] R. Hanbury Brown and R. Q. Twiss, Nature **177**, 27 (1956).
 - [7] P. Mehta, J. Samuel, and S. Sinha, Phys. Rev. A **82**, 034102 (2010).
 - [8] W. Tittel and G. Weihs, Quant. Inf. Comp. **1**, 3 (2001).
 - [9] M. A. Nielsen and I. L. Chuang, *Quantum Computation and Quantum Information*, 10th ed. (Cambridge University Press, Cambridge, 2010).
 - [10] M. Büttiker, Phys. Rev. Lett. **68**, 843 (1992).
 - [11] Y. Aharonov and D. Bohm, Phys. Rev. **115**, 485 (1959).
 - [12] I. Neder, N. Ofek, Y. Chung, M. Heiblum, D. Mahalu, and V. Umansky, Nature **448**, 333 (2007).
 - [13] P. Samuelsson, E. V. Sukhorukov, and M. Büttiker, Phys. Rev. Lett. **92**, 026805 (2004).
 - [14] J. Splettstoesser, M. Moskalets, and M. Büttiker, Phys. Rev. Lett. **103**, 076804 (2009).
 - [15] M. Ericsson, D. Achilles, J. T. Barreiro, D. Branning, N. A. Peters, and P. G. Kwiat, Phys. Rev. Lett. **94**, 050401 (2005).
 - [16] F. T. Arecchi, Phys. Rev. Lett. **15**, 912 (1965).
 - [17] W. Martienssen and E. Spiller, Am. J. Phys. **32**, 919 (1964).

- [18] G. Scarcelli, A. Valencia, and Y. Shih, EPL (Europhys. Lett.) **68**, 618 (2004).
- [19] R. Loudon, *The Quantum Theory of Light*, 3rd ed. (Oxford University Press, Oxford, 2000).
- [20] J. Brendel, N. Gisin, W. Tittel, and H. Zbinden, Phys. Rev. Lett. **82**, 2594 (1999).
- [21] S. Tanzilli, A. Martin, F. Kaiser, M. P. De Micheli, O. Alibart, and D. B. Ostrowsky, to appear in Laser & Photonics Reviews (2011), 10.1002/lpor.201100010.